

Organic & Biomolecular Chemistry

Accepted Manuscript



This is an *Accepted Manuscript*, which has been through the Royal Society of Chemistry peer review process and has been accepted for publication.

Accepted Manuscripts are published online shortly after acceptance, before technical editing, formatting and proof reading. Using this free service, authors can make their results available to the community, in citable form, before we publish the edited article. We will replace this *Accepted Manuscript* with the edited and formatted *Advance Article* as soon as it is available.

You can find more information about *Accepted Manuscripts* in the [Information for Authors](#).

Please note that technical editing may introduce minor changes to the text and/or graphics, which may alter content. The journal's standard [Terms & Conditions](#) and the [Ethical guidelines](#) still apply. In no event shall the Royal Society of Chemistry be held responsible for any errors or omissions in this *Accepted Manuscript* or any consequences arising from the use of any information it contains.

ARTICLE

1,8-Naphthalimide derivatives: New leads against dynamin I GTPase activity

Cite this: DOI: 10.1039/x0xx00000x

Mohammed K. Abdel-Hamid,^a Kylie A. Macgregor,^a Luke R. Odell,^{a†} Ngoc Chau,^b Anna Mariana,^{b§} Ainslie Whiting,^b Phillip J Robinson^b and Adam McCluskey^{a*}

Received 00th January 2012,
Accepted 00th January 2012

DOI: 10.1039/x0xx00000x

www.rsc.org/

Fragment-based *in silico* screening against dynamin I (dynI) GTPase activity identified the 1,8-naphthalimide framework as a potential scaffold for the design of new inhibitors targeting the GTP binding pocket of dynI. Structure-based design, synthesis and subsequent optimization resulted in the development of a library of 1,8-naphthalimide derivatives, called the Naphthaladyn™ series, with compounds **23** and **29** being the most active (IC₅₀ of 19.1 ± 0.3 and 18.5 ± 1.7 μM respectively). Compound **29** showed effective inhibition of clathrin-mediated endocytosis (IC_{50(CME)} 66 μM). The results introduce **29** as an optimised GTP-competitive lead Naphthaladyn™ compound for the further development of naphthalimide-based dynI GTPase inhibitors.

Introduction

Endocytosis is an important physiological process by which extracellular materials (including hormones and nutrients) enter the cell through budding into the plasma membrane. The formation of the endocytic vesicle involves the complex interplay between a wide array of proteins that assist in membrane invagination and subsequent fission step that releases a new vesicle into the cell. One such protein is the large GTPase dynamin, which plays crucial roles in the catalysis of membrane fission during clathrin-mediated endocytosis (CME), a common endocytic mode using clathrin-coated vesicles. At a late stage of this process, dynamin assembles into helical collar or ring at the neck of the newly forming vesicle. GTP hydrolysis triggers a major conformational change within the dynamin macromolecular structure effecting bud fission and the generation of a free endocytic vesicle.¹ As a key player in biological vesicle scission, dynamin has been considered as an attractive drug target in the control of various diseases, including epilepsy,²⁻⁴ bone loss diseases,^{5,6} kidney diseases,^{7,8} and the spread of infectious diseases.^{9,10}

Dynamin is a cytosolic protein composed of five domains: an amino-terminal G domain that binds and hydrolyses GTP; a middle domain or a stalk region which is involved in self-assembly and oligomerisation; a pleckstrin homology (PH) domain which interacts with the plasma membrane and induces the hemifission state; a GTPase effector domain (GED) which is also involved in self-assembly; and a proline-rich carboxy terminal domain (PRD) that interacts with SH3 domains in accessory proteins.¹¹⁻¹⁵ In mammals there are three dynamin genes which share the same domain organisation and 80% of

the overall protein sequence, although each shows a distinct tissue expression pattern.¹ Dynamin I (dynI) is mainly found in neurons while dynamin II (dynII) is ubiquitously expressed and dynamin III (dynIII) is found in the brain (at much lower levels than dynI), testis and the lung.^{13,16} Each gene can functionally replace the others for CME, but not for all other known cellular functions of dynamin.¹⁷⁻¹⁹

Our laboratory has reported the identification and development of many discrete families of small molecule inhibitors of the GTPase activity of dynI including the MiTMAB,²⁰ Bis-T,^{21,22} RTIL,²³ Iminodyn™,²⁴ Pthaladyn™,²⁵ Dyngo™,^{26,27} Rhodadyn™,²⁸ Quinodys™,²⁹ series two generations of Dynole™,^{30,31} and the clinically used antipsychotic compounds.³² Each series inhibits dynamin by different molecular mechanisms, with only the Pthaladyns, Quinodys and some Pyrimidin series being known to be directly targeting the GTP binding site in the G domain.^{9,33} Herein we use a combined technique of fragment-based virtual screening, structure-based design based on the 1,8-naphthalimide, which we call the Naphthaladyn™, scaffold and focused library synthesis to develop a new class of dynI GTPase inhibitors engineered to target the GTP binding pocket of dynI.

Results and Discussion

To produce novel compounds that target the GTP-binding pocket of the dynI G domain, the initial design process commenced with the virtual screening of our in-house fragment library against the GTP binding pocket of dynI (PDB code: 3ZYC),¹¹ using Multiple Copy Simultaneous Search (MCSS) docking software.³⁴ The preliminary screening identified the 1,8-naphthalimide framework as a potential scaffold.

Examination of naphthalimide clusters inside the GTP binding pocket showed varied orientations in which the docked fragments were able to establish both hydrophobic and hydrogen bond contacts with the pocket residues (Supporting information, Figure S1). The Gaussian contact surface for the GTP binding pocket was calculated in order to guide subsequent synthetic efforts through the identification of possible substitution pattern for the naphthalimide fragment (Figure 1). The highest ranked fragment pose showed the orientation of the naphthyl moiety in close proximity to the position of the magnesium ion inside the pocket. This suggested the possibility of incorporating a metal coordinating group into the naphthalimide ring that could mimic the interaction between the magnesium ion and the nucleotide phosphate group in GTP. Sulfate, sulfonyl, sulfamyl groups and their derivatives are known successful phosphate bioisosteres that are not based on phosphorus.³⁵⁻³⁷ The geometry of these fully oxidised sulphur-containing groups

shows an approximate tetrahedral arrangement which is similar to the shape of the phosphate groups.³⁷ For synthetic tractability we envisaged the introduction of a sulfonate moiety to the naphthyl ring as a potential phosphate bioisostere. The Gaussian surface suggested scope for the introduction of a N-imide hydrophobic moiety to target the hydrophobic region identified between the G4 residues (Lys206 and Leu209) and the “dynamamin specific loop” residues (Val35 and Ser238) at the pocket entrance (Figure 1). Hydrophilic amino acids at the pocket entrance (Asp208, Asn236 and Arg237) can be targeted by the incorporation of a hydrogen bond donor/acceptor group into the introduced N-imide hydrophobic moiety. Hydrogen bonding interactions with amino acids at the P-loop and switch I region of the pocket could be achieved either by the naphthalimide ring carbonyl moieties or through the introduction of an additional hydrogen bond donor/acceptor on the naphthalene ring.

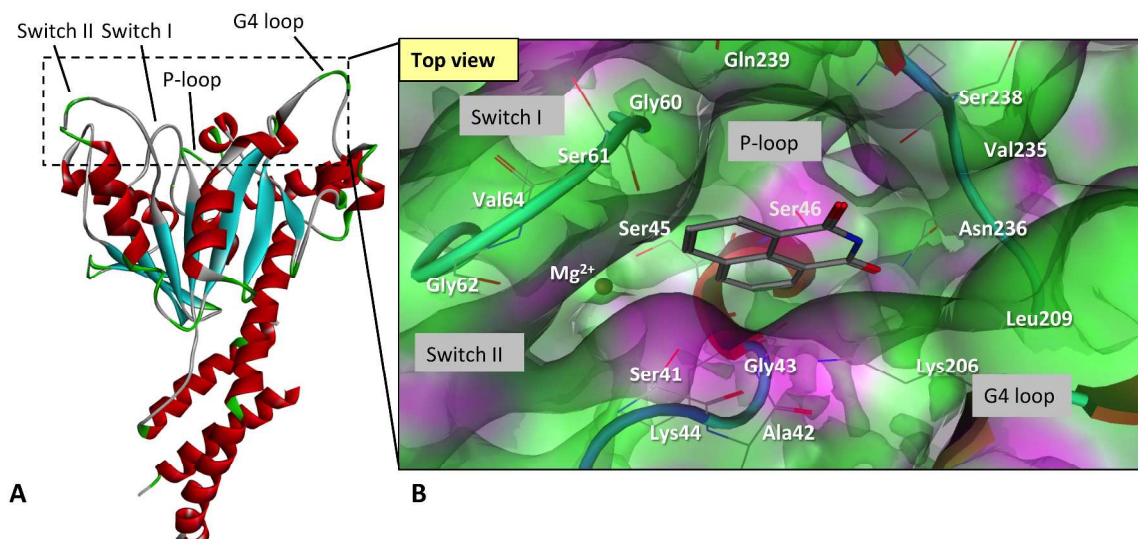
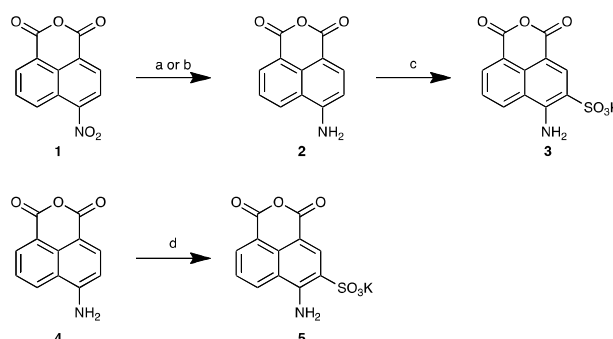


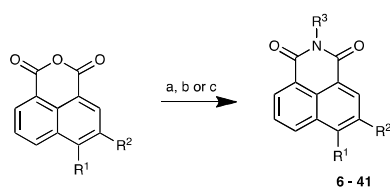
Figure 1. (A) A ribbon representation for dyln GTPase domain, important loops close to the GTP binding site are labelled. (B) Gaussian contact surface of the dyln GTP binding site (green for hydrophobic and purple for hydrophilic) showing the docked naphthalimide fragment (stick representation).

Based on our molecular modelling observations, a library of 1,8-naphthalimide derivatives was designed (see Table 1 for details) and synthesised as shown in Scheme 1. The key intermediate **3** was accessed by the reduction of the commercially available 3-nitro-1,8-naphthalic anhydride (**1**) followed by sulfonation. The anhydride **1** was reduced to the corresponding amine **2** either classically using stannous chloride in acidic medium⁸ or by flow hydrogenation approaches (ThalesNano H-cube[®] using 10% Pd/C). The flow reduction approach afforded both a higher yield and simpler work up of **2**. Sulfonation of **2** with fuming sulfuric acid at 50 °C followed by treatment with aqueous KCl gave precipitate of the potassium salt (**3**). Sulfonation of 1,8-naphthalic anhydride (**4**) at 120°C gave **5** in a 96% yield.



Scheme 1. Synthesis of 1,8-naphthalimide derivatives. Reagents and conditions: (a) ThalesNano H-Cube[®], 10% Pd/C, THF, 40°C, 10 bar, 1 mL.min⁻¹, 2 cycles; (b) SnCl₂, HCl, ethanol, reflux 2 hr; (c) *i.* Fuming sulfuric acid, 50°C, 3 hr, *ii.* Saturated aq. KCl, room temperature; (d) *i.* Fuming sulfuric acid, 120°C, 1 hr, *ii.* Saturated aq. KCl, RT.

With the substituted naphthalimides (**2-5**) in hand, the *N*-imide substituted analogues were derived through condensation with the desired amine (Scheme 2). The anhydride-amine condensation procedure was amine dependent, with each amine requiring subtle protocol optimisation to afford useful yields. Typically with neutral aliphatic amines, the corresponding analogues were prepared via simple condensation of the anhydride derivative with a slight excess of the amine in the presence of a catalytic amount of triethylamine (TEA). The same reaction conditions with aniline resulted in low levels of product (<10%; as evidenced from ¹H-NMR analysis). Adaptation of the Lucifer Yellow synthesis using 2 equivalents of the desired aniline in a 5% acetic acid solution followed by treatment with KCl gave the desired analogues, as potassium salts, in good to high yields (60-76%).³⁹ All other *N*-substituted analogues were synthesised using 2 equivalents of amine in a lithium acetate pH 5 buffer (see Experimental).



Scheme 2. a) Amine derivative (see Tables 1 and 2 for details), TEA, Ethanol, 100°C (sealed tube), 18 hr; b) Amine derivative, 1 M Li⁺/H⁺ acetate, pH 5, 130°C, 18 hr; c) i. Amine derivative, 5% acetic acid, 130°C, 18 hr, ii. Saturated aq. KCl, 4°C, 12 hr.

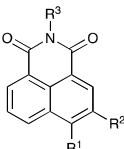
The synthesised 1,8-naphthalimide derivatives (**6-18**) were evaluated for their ability to inhibit the GTP hydrolysis activity of dynI stimulated by L-phosphatidylserine (PS) liposomes (Table 1).

Promising levels of dynI inhibitory activity was evident for those analogues with sulfonate and amino substituted naphthalimide rings (**9-18**; excepting **10** and **14** which were inactive). This is consistent with the modelling predicted role for the sulfonate moiety as a Mg²⁺ coordinator within the GTP binding pocket. The presence of an amino group adjacent to the sulfonate group significantly promotes this role, leading to an enhancement in the inhibitory activity (**7**, not active at 300 μM, vs. **9**, IC₅₀ = 193 μM).

The presence of a terminal hydrogen bonding group on the *N*-imide substituent was important for dynI inhibitory activity with **9**, **11** and **16** displaying higher levels of dynI inhibition than the corresponding non-hydrogen bonding analogues **10** and **18**, which were essentially inactive. However, analogues **12** and **14** showed no activity despite of the presence of a terminal primary/secondary amino group, suggesting that the interaction between the enzyme and this terminal moiety is dependent on pK_a. This was evidenced by the activity trend for analogues **11**, **9**, **12** and **14**, while an increase of the inhibitory activities is observed as the acidity of the terminal moiety increases. While the modeling analysis suggested enhanced interactions for the *N*-aromatic imide substituted naphthalimides (**15-18**), this was not reflected in the observed

dynI IC₅₀ values which ranged from not active (**18**) to very low levels of activity.

Table 1. Inhibition of PS-stimulated dynI GTPase activity by 1,8-naphthalimide analogues **6-18** up to a maximum of 300 μM of each compound.



Compound	R ¹	R ²	R ³	DynI IC ₅₀ (μM)
6	H	H		NA ^a
7	H	SO ₃ K		>>300 μM ^a
8	SO ₃ K	H		>>300 μM ^a
9	NH ₂	SO ₃ K		193 ± 37 ^a
10	NH ₂	SO ₃ K		NA ^a
11	NH ₂	SO ₃ K		94 ^a
12	NH ₂	SO ₃ K		>300 μM ^a
13	NH ₂	SO ₃ K		509 ^a
14	NH ₂	SO ₃ K		NA ^a
15	NH ₂	SO ₃ K		>>300 μM ^a
16	NH ₂	SO ₃ K		159 ± 22 ^a
17	NH ₂	SO ₃ K		296 ± 48 ^a
18	NH ₂	SO ₃ K		NA ^a

NA = not active up to 300 μM; ^a n=1, mean ± 95% CI of triplicate; ^b n=2, mean ± SEM of independent experiments, triplicate data points.

In order to explain the observed biological data and to explore potential naphthalimide modifications for enhanced dynI inhibition, the tested compounds (**6-18**) were docked into the GTP binding pocket of dynI (PDB code: 3ZYC) using the docking engine of Molecular Operating Environment (MOE) software.⁴⁰ This revealed a similar orientation for all the active compounds in the binding pocket, in agreement with the initial proposed orientation for the 1,8-naphthalimide fragments. Closer inspection of the predicted docked pose of the most active analogue, **11**, shows the close proximity of the sulfonate group to the magnesium ion, allowing the possibility of double coordination (Figure 2). In this binding pose the sulfonate group could also participate in a range of either direct or water-bridged hydrogen bonding interactions with amino acids in the switch I and switch II region binding pocket. The adjacent amino group acts as a hydrogen bond donor to either the backbone of Gly62 or the side chain of Ser41 through a bridging water molecule. This interaction was considered to be critical, while Gly62 and Ser41 are playing important role in stabilising the P-loop and switch I conformations, such that

they are poised for catalysis.⁴¹ Other significant predicted interactions involved the hydrogen bonding between the terminal carboxyl group and the backbone of Arg237 which

highlights the importance of a hydrogen bond donor at the imide nitrogen substituent for enhanced dynI inhibitory activity.

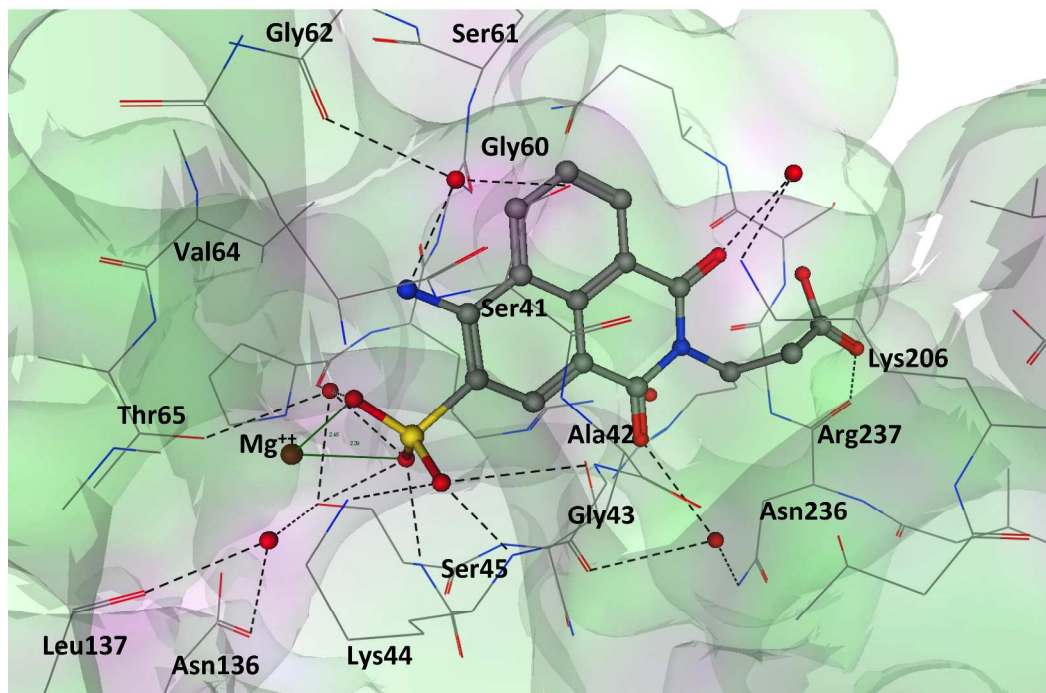


Figure 2. A molecular modelling representation of the predicted binding pose of naphthalimide **11** (ball and stick) within the GTP binding pocket of dynI (PDB 3ZYC). Potential hydrogen bond interactions are shown as dashed lines and the sulfonate-Mg²⁺ coordination interactions are shown by the green lines.

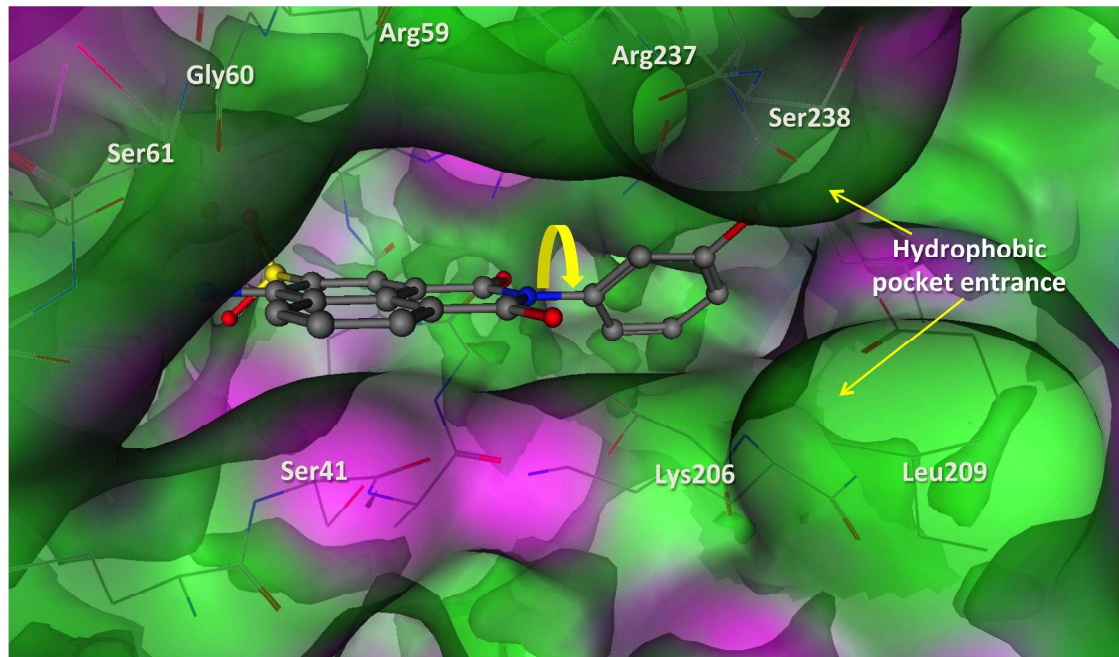


Figure 3. A 3D representation for the docked **16** (ball and stick) into the GTP binding pocket (Gaussian surface). Lack of terminal phenyl flexibility (yellow curved arrow) leads to loss of proper hydrophobic interactions with amino acids at the pocket entrance.

The unexpected lower activity of the aromatic group bearing analogues (**15-18**) was examined through evaluation of the predicted binding pose of **16** within the GTP binding site of

dynI (Figure 3). The docked pose of **16** shows a clear deviation from planarity of the N-imide phenyl moiety, to such an angle that prevents proper engagement with the key hydrophobic

moieties at the pocket entrance (Lys206, Leu209 and Val235). This suggested that introduction of a spacer group between the imide and aromatic moiety would be required to enhance the aromatic moiety engagement with the pocket entrance hydrophobic residues.

Table 2. Inhibition of PS-stimulated dynI GTPase activity by 1,8-naphthalimide analogues **19-30**.

Compound	R ³	DynI IC ₅₀ (μM)
19		93 ± 13 ^a
20		62 ± 11 ^a
21		113 ± 12 ^a
22		NA ^a
23		19.1 ± 0.3 ^b
24		70.3 ± 17 ^c
25		155 ± 47 ^a
26		88 ^a
27		123 ± 48 ^a
28		44.8 ± 4.1 ^b
29		18.5 ± 1.7 ^c
30		NA ^c

NA = not active up to 300 μM; ^a n=1, mean ± 95% CI of triplicate; ^b n=2, ^c n=3, mean ± SEM of independent experiments, triplicate data points.

A second 1,8-naphthalimide analogue library of (**19-30**) was designed, guided by the biological activity obtained by the first library and the molecular modelling predicted docking poses (Table 2). The synthesis was conducted using the same general procedure described in Scheme 2. The desired analogues were isolated in good yields and high purity.

Biological evaluation of the new analogues revealed an overall improvement in activity with two analogues **23** and **29** returning dynI IC₅₀ of 19.1 and 18.5 μM, respectively (Table 2). The data emphasised that the presence of a hydrogen bond donating group was critical for the activity of analogues containing aliphatic substituents. Consistently with the modelling study, the introduction of a methylene group between the terminal aromatic moiety and the imide nitrogen provided sufficient substituent flexibility to engage with the key residues within the GTP binding pocket. The effect of increased flexibility is most clearly evident on comparison of **15** and **24** (dynI IC₅₀ >>300 μM vs. 70.3 μM), **17** and **28** (dynI

IC₅₀ 296 μM vs. 44.8 μM). Increasing the length of the spacer moiety from methylene to ethylene resulted in a complete abolishment of activity from an IC₅₀ value of 70.8 μM (**24**) to inactive (**30**) against dynI. The good activity shown by the unsubstituted analogue **24** suggests that hydrophobic and/or cation-arene interactions between the phenyl ring and the binding site more than adequately compensate for the loss of possible hydrogen bond interactions. The data also supports the assumption that increasing the acidity of the terminal hydrogen bond donating moiety corresponds to an increase in potency (**26-29**).

Docking of **29** into dynI GTP binding site (Figure 4A) revealed similar orientation for the naphthalimide moiety compared to the docked **16** (Figure 3). However, the introduction of a methylene group between the phenyl ring and the imide nitrogen makes it possible for the terminal phenyl ring to engage in hydrophobic as well as cation-arene interactions at the pocket entrance (ESI Figure S2). The carboxyl group is involved in two hydrogen bond interactions at the G4 loop of the pocket through residues Lys206 and Asp208 in addition to accepting a hydrogen bond from Asn236 at the opposite side of the pocket entrance (Figure 4B).

Inhibition of dynamin should also inhibit CME if the compound is cell permeable and not rapidly degraded in cells. The two most active 1,8-naphthalimide analogues against dynI **23** and **29** were therefore tested for the inhibition of CME by the quantification of their ability of inhibiting the internalisation of fluorescently conjugated transferrin (Tfn-A594) into U2OS osteosarcoma cells (Table 3). Both naphthalimide analogues inhibited CME, which is likely to be mediated by dynII in these cells. The lower activity of **23** may potentially be attributed to cell permeability problems as a result of the low lipophilic characters of **23** compared to **29**.

Table 3. Clathrin-mediated endocytosis (CME) inhibition of Tfn-A594 in U2OS cells for selected naphthalimide-based dynI inhibitors.

Compound	CME IC ₅₀ (μM)
23	115
29	66

n=1, triplicate data points.

Conclusions

Given that the design and synthesis of ATP-binding site directed protein kinases inhibitors has resulted in remarkable potency, selectivity and efficacy in humans,⁴² our long-term goals are to design GTP-binding site directed dynamin GTPase inhibitors. Using a *de novo* structure- and fragment-based strategy we successfully identified a new series of GTP-binding pocket-directed dynI GTPase inhibitors based on the 1,8-naphthalimide scaffold, i.e. the NaphthaladynTM series. Synthesis and testing of the first designed library (**6-18**) showed promising activity against dynI with **11** showing IC₅₀ of 94 μM. Further structural optimisation using molecular modeling together with studying the structure-activity relationship data for the first library resulted in the design and synthesis of a second library (**19-30**) with more than 5 times enhancement in

activity. Two analogues (**23** and **29**) were selected to test the ability of dynI GTPase inhibitors based on the naphthalimide scaffold to inhibit the activity of dynamin in cells as indicated by inhibiting CME. The results showed consistent activity with the dynI GTPase inhibition data while analogue **29** showed the

highest activity in both assays (dynI GTPase IC₅₀ of 18.5 and IC_{50(CME)} of 66 μM). Analogue **29** is an optimised lead compound for the further development of naphthalimide-based dynI GTPase inhibitors.

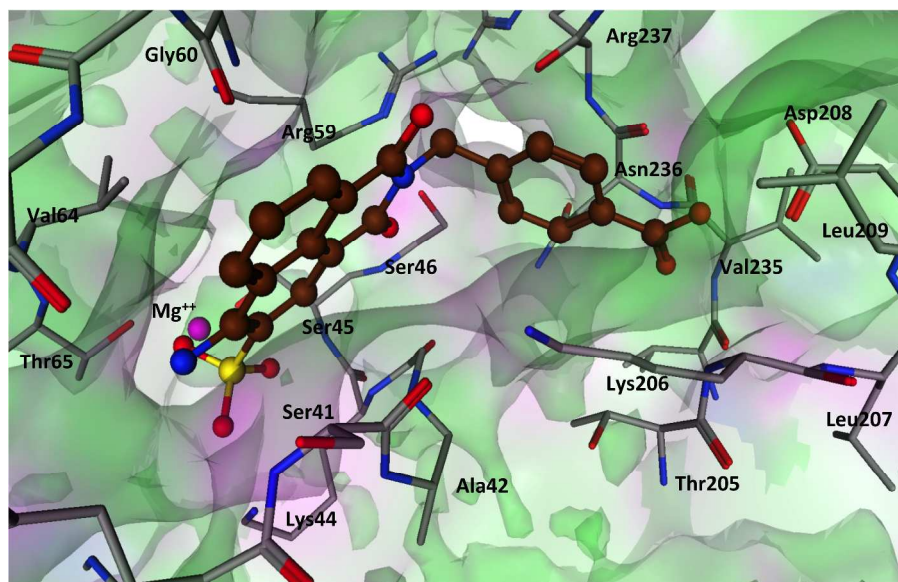


Figure 4. 3D representation for the predicted orientation of **29** (carbon atom in brown, ball and stick representation) at the GTP binding pocket (selected residues are shown in stick representation and Mg²⁺ is shown in pink ball representation).

Experimental

Fragment-based Docking

Molecular modeling studies were performed using the crystal structure of dynI GTPase domain bound to GMPPCP ligand (PDB code: 3ZYC).¹¹ The pdb file was imported into Accelrys Discovery Studio package and the ligand binding pocket was assigned before the ligand was omitted. A library of in-house fragments and the Maybridge Ro3 fragment library ($n \approx 200$, MW < 250, cLogP < 3, flexibility index < 3, number of hydrogen bond acceptors ≤ 3 and number of hydrogen bond donors ≤ 2) was docked into the assigned binding site using Multiple Copy Simultaneous Search (MCSS) software. The highest ranked fragments were collected and retained for further development.

Molecular Docking

Molecular docking simulations were performed using the docking engine of Molecular Operating Environment (MOE) software.⁴⁰ The designed 3D structures were built using the software molecular builder and were subjected to conformational analysis using stochastic search approach. Each conformational library was docked into the GTP binding pocket using “Triangle Matcher” as the placement method and “London dG” as the scoring function. The highest ranked pose for each compound was relaxed in the binding pocket using LigX energy minimisation and the obtained complex was inspected for potential interactions.

Dynamain GTPase assay

Phosphatidylserine (PS), phenylmethylsulfonyl fluoride (PMSF) and Tween 80 were from Sigma Aldrich (St. Louis, MO). GTP was from Roche Applied Science (Basel, Switzerland) and leupeptin was from Bachem (Bubendorf, Switzerland). All other reagents were of analytical reagent grade or better.

Compounds were made up as stock solutions of 30 mM in 100% DMSO and further diluted in assay buffer such that the final DMSO concentration was at most 3.3% (dynI GTPase activity was unaffected by DMSO up to this concentration). Compounds were made up fresh from powder stock just prior to commencing of assay and stock solutions were stored at -20 °C for several months.

Native endogenous dynI was purified from sheep brain by extraction from the peripheral membrane fraction of whole brain,²⁴ and affinity purification on GST-Amph2-SH3-sepharose as previously described,⁴³ yielding 8-10 mg of protein from 250 g of sheep brain.

The Malachite Green method was used for the sensitive colorimetric detection of orthophosphate (P_i) release from GTP as previously described.²⁴ Briefly, GTPase activity was stimulated on 20-30 nM dynI by 4 μg/mL sonicated PS liposomes, in the presence of 1 μg/mL leupeptin, 0.1 mM PMSF, 0.3 mM GTP and test compound for 30 min at 37 °C in a final assay volume of 150 μL. The reaction was terminated with 10 μL of 0.5 M EDTA (pH 7.4) and phosphate was detected by addition of Malachite Green solution (40 μL: 2% w/v ammonium molybdate tetrahydrate, 0.15% w/v Malachite Green and 4 M HCl) for 5 min. Data analysis and IC₅₀ values

estimation were calculated in Microsoft Excel and GraphPad Prism v5.0, using non-linear regression methods.

CME Assay

Fibronectin and DAPI were from Sigma Aldrich (St. Louis, MO). Paraformaldehyde (PFA) was from BDH (AnalaR Merck Chemicals, Darmstadt, Germany). Phosphate buffered saline (PBS), foetal bovine serum (FBS) and Dulbecco's Minimal Essential Medium (DMEM) were from Invitrogen (Paisley, Strathclyde, UK). Alexa-594 conjugated Transferrin (Tfn-A594) was from Molecular Probes (Eugene, OR, USA). All other reagents were of analytical grade or better.

CME was examined by a high throughput, quantitative assay for measuring Tfn uptake in U2OS osteosarcoma cells, based on methods described previously.³³ Briefly, cells were cultured on fibronectin-coated 96-well glass-bottomed plate, maintained in DMEM supplemented with 10% FBS at 37°C in 5% CO₂. Cells were then serum-starved overnight (16 hr) before being treated with test compounds or vehicle (1% DMSO) for 30 min at 37°C. Tfn-A594 (4 µg/mL) was applied for 8 min at 37°C and endocytosis was being arrested by placing the cells on ice (4°C). Surface bounded Tfn was removed with an ice-cold acid wash solution (0.2 M acetic acid, 0.5 M NaCl, pH 2.8) for 10 min followed by an ice-cold PBS wash for 5 min. Cells were immediately fixed with 4% PFA for 10 min at room temperature. Nuclei were labeled with DAPI stain solution. Cells imaging and data analysis were done by a high content imaging system MetaXpress (Molecular Devices). Quantitative analysis of Tfn-A594 uptake in U2OS cells was performed by high content imaging. Nine images were collected from each well, averaging 40-50 cells per image, totaling of ~1,200 cells per condition. IC₅₀ values were calculated using Graphpad Prism 5, where data was expressed as percentage of control cells (vehicle treated).

Chemistry

General Methods

All reactions were performed using standard laboratory equipment and glassware. Solvents and reagents were purchased from Sigma Aldrich, Lancaster International or TCI and used as received. Organic solvents were bulk quality, and were distilled from glass prior to use. Organic solvent extracts were dried with magnesium sulfate (MgSO₄), and dried under reduced pressure with either Büchi or Heidolph rotary evaporators. Melting points were recorded in open capillaries on a Stuart SMP11 Melting Point Apparatus. Temperatures are expressed in degrees Celsius (°C). Where available, literature values are provided and appropriately referenced. Electrospray mass spectra were recorded using 10% DMSO/H₂O or HPLC-grade methanol or acetonitrile as carrier solvents on a Shimadzu LC-MS spectrometer.

Nuclear magnetic resonance (NMR) spectroscopy was performed on a Bruker Avance 300 MHz spectrometer, where proton NMR (¹H-NMR) spectra and carbon NMR (¹³C-NMR) spectra were acquired at 300 and 75 MHz respectively, or a Bruker Avance III 400 MHz spectrometer, where ¹H-NMR and

¹³C-NMR were acquired at 400 and 100 MHz respectively. All spectra were recorded in deuterated dimethyl sulfoxide (DMSO-*d*₆), obtained from Sigma Aldrich or Cambridge Isotope Laboratories Inc., unless otherwise stated, with the residual solvent peaks used as the internal reference (δ 2.49 (quintet) and δ 39.7 (septet) for ¹H-NMR and ¹³C-NMR respectively). Chemical shifts (δ) were measured in parts per million (ppm) and referenced against the internal reference peaks. Coupling constants (*J*) were measured in Hertz (Hz).

NMR assignments were determined through the interpretation of one- and two-dimensional spectra, specifically gradient heteronuclear single quantum correlation (gHSQC), gradient heteronuclear multiple bond correlation (gHMBC) and distortionless enhancement by polarization transfer quaternary (DEPTQ) spectroscopy. Multiplicities are denoted as singlet (s), broad singlet (br s), doublet (d), doublet of doublets (dd), doublet of doublet of doublets (ddd), triplet (t), triplet of doublets (td), doublet of triplets (dt), quartet (q), quintet (quin) and multiplet (m). Peaks are listed in increasing chemical shift in the following format: chemical shift (integration (¹H), multiplicity (¹H), coupling constant (¹H), ascribed assignment).

4-Amino-1,8-naphthalic anhydride (2)

Method 1

A solution of tin (II) chloride (4.015 g, 21.2 mmol) in concentrated HCl (32 %, 3.5 mL) was added dropwise to a stirring suspension of 4-nitro-1,8-naphthalic anhydride (**1**) (1.009 g, 4.1 mmol) in ethanol (2 mL), and the resulting suspension stirred at reflux for 2 hours. The resulted mixture was cooled to room temperature and the precipitated product was collected by filtration, washed sequentially with water, ethanol and ether, and dried under vacuum. An orange-red solid was obtained.

Yield 0.761 g (86 %); MP > 250 °C (Lit. > 300 °C).³⁸ ¹H NMR δ 6.86 (1H, d, *J* = 8.4 Hz), 7.67 (1H, dd, *J* = 7.2, 8.4 Hz), 7.77 (2H, br s, NH₂), 8.17 (1H, d, *J* = 8.4 Hz), 8.42 (1H, dd, *J* = 0.9, 7.2 Hz), 8.67 (1H, dd, *J* = 0.9, 8.4 Hz); ¹³C NMR δ 102.4, 108.9, 118.5, 119.5, 124.6, 130.9, 132.8, 133.2, 136.1, 154.1, 160.5, 162.2; MS (ESI-) *m/z*: 212 (100%, M - H).

Method 2

A solution of 4-nitro-1,8-naphthalic anhydride (**1**) (0.50 g, 2.1 mmol) in dry THF (20 mL) was connected to the sample inlet line of the ThalesNano H-cube[®] flow hydrogenation reactor. "Full Hydrogen" mode was selected using 10% Pd/C catalyst cartridge. The solution was injected into the reactor at a rate of 1 mL.min⁻¹ under a pressure of 10 bar while adjusting the temperature at 40°C. The reaction mixture was collected and recirculated through the reactor for a second pass under the same conditions. The collected solution was evaporated to dryness affording 0.37 g (98 %) of the desired product (**2**) with identical physical and spectral properties to what was obtained in *Method 1*.

4-Amino-3-sulfo-1,8-naphthalic anhydride, potassium salt (3)

4-Amino-1,8-naphthalic anhydride (**2**) (0.204 g, 1.0 mmol) was dissolved in fuming sulfuric acid (4 mL) and the resulting

solution stirred at 50 °C for 3 hours. The mixture was then cooled to room temperature, and poured into water (20 mL). Aqueous saturated potassium chloride (25 mL) was then added, resulting in the precipitation of the off-yellow product. The product was collected by filtration, washed sequentially with water, ethanol and ether, and dried under vacuum.

Yield 0.248 g (78 %); MP > 250 °C; ¹H NMR δ 7.72 (1H, dd, *J* = 7.2, 8.4 Hz), 8.07 (2H, br, s, NH₂), 8.43 (1H, dd, *J* = 0.9, 7.2 Hz), 8.57 (1H, s), 8.78 (1H, dd, *J* = 0.9, 8.4 Hz); ¹³C NMR δ 102.1, 118.9, 121.1, 125.4, 125.9, 131.6, 132.7, 133.5, 134.6, 149.7, 160.8, 162.3; MS (ESI-) *m/z*: 291 (100%, M – K).

3-Sulfo-1,8-naphthalic anhydride, potassium salt (5)

1,8-Naphthalic anhydride (0.990 g, 5.0 mmol) was dissolved in fuming sulfuric acid (6 mL). The resulting solution was stirred at 120 °C for 1 hour (until a drop of the mixture, when added to water, did not precipitate), then cooled to room temperature. The cooled solution was then poured into water (30 mL). Addition of aqueous saturated potassium chloride (30 mL) resulted in precipitation of the product. The white solid was collected by filtration, washed sequentially with water, ethanol and ether, and dried under vacuum.

Yield 1.580 g (96 %); MP > 250 °C; ¹H NMR δ 7.91 (1H, dd, *J* = 7.2, 8.4 Hz), 8.51 (1H, dd, *J* = 0.9, 7.2 Hz), 8.62 (1H, d, *J* = 1.5 Hz), 8.64 (1H, dd, *J* = 0.9, 8.4 Hz), 8.73 (1H, d, *J* = 1.5 Hz); ¹³C NMR δ 119.7, 128.4, 130.0, 130.3, 131.4, 131.6, 133.1, 136.5, 147.7, 161.1, 161.2; MS (ESI-) *m/z*: 277 (100%, M – K).

N-(2-Hydroxyethyl)-1,8-naphthalimide (6)

Ethanolamine (350 μL, 5.8 mmol) was added dropwise to a stirring suspension of 1,8-naphthalic anhydride (1.005 g, 5.1 mmol) in ethanol (20 mL). The resulting suspension was heated under reflux for 18 hours, then allowed to cool to room temperature. The precipitated product was collected by filtration, washed with ethanol, then ether, and dried under vacuum to afford a yellow-brown solid.

Yield 0.994 g (81 %); MP 174-176 °C (Lit. 172-174 °C; 173-175 °C; 175-176 °C);⁴⁴⁻⁴⁶ ¹H-NMR δ 3.61 (2H, m, H₂), 4.14 (2H, t, *J* = 6.6 Hz, H₁), 4.81 (1H, t, *J* = 6.0 Hz, OH), 7.85 (2H, dd, *J* = 7.5, 8.1 Hz, H₃, H₆), 8.44 (2H, dd, *J* = 0.9, 8.1 Hz, H₄, H₅), 8.47 (2H, dd, *J* = 0.9, 7.5 Hz, H₂, H₇); ¹³C-NMR δ 42.0 (C₁), 58.0 (C₂), 122.4 (C₁, C₈), 127.4 (C₃, C₆), 127.6 (C_{8a}), 130.8 (C₂, C₇), 131.5 (C_{4a}), 134.4 (C₄, C₅), 163.7 (C₉, C₁₀); MS (ESI-) *m/z*: 240 (M – H).

3-Sulfo-*N*-(2-hydroxyethyl)-1,8-naphthalimide, potassium salt (7)

Synthesised using the same general procedure as for **6**, commencing with 3-sulfo-1,8-naphthalic anhydride (potassium salt) and ethanolamine. A pale yellow solid was obtained.

Yield 0.160 g (71 %); MP > 250 °C; ¹H NMR δ 3.62 (2H, m), 4.15 (2H, t, *J* = 6.6 Hz), 4.81 (1H, t, *J* = 6.0 Hz, OH), 7.87 (1H, dd, *J* = 7.5, 8.1 Hz), 8.46 (1H, dd, *J* = 0.9, 7.5 Hz), 8.54 (1H, dd, *J* = 0.9, 8.1 Hz), 8.65 (1H, d, *J* = 1.5 Hz), 8.66 (1H, d, *J* = 1.5 Hz); ¹³C NMR δ 42.1, 58.0, 122.3, 122.4, 127.4, 127.8, 128.6, 130.0, 131.1, 135.1, 147.1, 163.6, 163.8 ppm; MS (ESI-)

m/z: 320 (M – K) (100 %); Elem. Anal. (C₁₄H₆KNO₆S): Calc. C 46.79, H 2.80, N 3.90; Found C 46.90, H 2.97, N 3.88.

4-Sulfo-*N*-(2-hydroxyethyl)-1,8-naphthalimide, potassium salt (8)

Synthesised using the same general procedure as for **6**, commencing with 4-sulfo-1,8-naphthalic anhydride (potassium salt) and ethanolamine. A white solid was obtained.

Yield 0.177 g (77 %); MP > 250 °C; ¹H NMR δ 3.62 (2H, m), 4.15 (2H, t, *J* = 6.6 Hz), 4.82 (1H, t, *J* = 6.0 Hz, OH), 7.87 (1H, dd, *J* = 7.2, 8.7 Hz), 8.20 (1H, d, *J* = 7.5 Hz), 8.45 (1H, d, *J* = 7.5 Hz), 8.48 (1H, dd, *J* = 1.2, 7.2 Hz), 9.23 (1H, dd, *J* = 1.2, 8.7 Hz); ¹³C NMR δ 42.1, 58.0, 122.4, 123.0, 125.1, 126.9, 127.7, 128.3, 130.2, 130.5, 134.2, 149.9, 163.5, 163.9; MS (ESI-) *m/z*: 320 (M – K) (100 %); Elem. Anal. (C₁₄H₁₀KNO₆S·H₂O): Calc. C 44.55, H 3.20, N 3.70; Found C 44.39, H 3.07, N 3.61.

4-Amino-3-sulfo-*N*-(2-hydroxyethyl)-1,8-naphthalimide, potassium salt (9)

To a stirred suspension of 4-amino-3-sulfo-1,8-naphthalic anhydride, potassium salt (**3**) (0.199 g, 0.6 mmol), in 1 M Li⁺/H⁺ acetate pH 5 buffer (5 mL), was added ethanolamine (200 μL, 3.3 mmol). The reaction mixture was stirred at 120 °C for 18 hours, then diluted to 20 mL with hot water. Addition of KCl (~0.5 g), followed by cooling to 4 °C, resulted in precipitation of the product. The resulting suspension was then stored at 4 °C for 24 hours. The solid product was collected by filtration, washed sequentially with water, ethanol and ether, and dried under vacuum. A bright yellow solid was obtained.

Yield 0.137 g (61 %); MP > 250 °C; ¹H NMR (DMSO-*d*₆) δ 3.57 (2H, m, H₂), 4.11 (2H, t, *J* = 6.6 Hz, H₁), 4.80 (1H, t, *J* = 6.0 Hz, OH), 7.68 (1H, dd, *J* = 7.2, 8.4 Hz, H₆), 7.80 (2H, br, s, NH₂), 8.41 (1H, dd, *J* = 1.2, 7.2 Hz, H₇), 8.62 (1H, s, H₂), 8.69 (1H, dd, *J* = 1.2, 8.4 Hz, H₅); ¹³C NMR (DMSO-*d*₆) δ 41.6 (C₁), 58.1 (C₂), 106.9 (C₁), 120.8 (C_{4a}), 122.1 (C₈), 124.7 (C₆), 125.1 (C₃), 129.7 (C_{8a}), 129.9 (C₅), 131.2 (C₇), 132.8 (C₂), 148.3 (C₄), 163.2 (C₁₀), 164.1 (C₉) ppm; MS (ESI-) *m/z*: 335 (M – K) (100 %). HRMS (ESI-) *m/z* calculated for C₁₄H₁₁KN₂O₆S (M – K) 335.0343 found 335.0339.

4-Amino-3-sulfo-*N*-(2-methoxyethyl)-1,8-naphthalimide, potassium salt (10)

Synthesised using the same general procedure as for **6**, commencing with 4-amino-3-sulfo-1,8-naphthalic anhydride, potassium salt (**3**) and 2-methoxyethylamine. A yellow solid was obtained.

Yield 0.209 g (77 %); MP > 250 °C; ¹H NMR δ 3.24 (3H, s), 3.54 (2H, t, *J* = 6.3 Hz), 4.21 (2H, t, *J* = 6.3 Hz), 7.68 (1H, dd, *J* = 7.2, 8.4 Hz), 7.85 (2H, br s, NH₂), 8.42 (1H, d, *J* = 7.2 Hz), 8.61 (1H, s), 8.72 (1H, d, *J* = 8.4 Hz); ¹³C NMR δ 38.4, 58.1, 69.0, 106.6, 120.8, 121.9, 124.7, 125.1, 129.7, 130.1, 131.3, 132.9, 148.4, 163.1, 164.0; MS (ESI-) *m/z*: 349 (M – K) (100 %). HRMS (ESI-) *m/z* calculated for C₁₅H₁₃N₂O₆S (M – K) 349.0500, found 349.0518.

4-Amino-3-sulfo-N-(2-carboxyethyl)-1,8-naphthalimide, potassium salt (11)

Synthesised using the same general procedure as for **9**, commencing with 4-amino-3-sulfo-1,8-naphthalic anhydride, potassium salt (**3**) and β -alanine. Total reaction time was 72 hours. A yellow-brown solid was obtained.

Yield 0.086 g (35 %); MP > 250 °C; $^1\text{H-NMR}$ δ 2.54 (2H, m), 4.23 (2H, m), 7.68 (1H, dd, $J = 7.2, 8.4$ Hz), 7.82 (2H, br s, NH_2), 8.42 (1H, dd, $J = 1.2, 7.2$ Hz), 8.61 (1H, s, H_2), 8.69 (1H, dd, $J = 1.2, 8.4$ Hz), 12.20 (1H, br s, COOH); $^{13}\text{C-NMR}$ δ 32.6, 35.6, 106.7, 120.8, 122.0, 124.7, 125.2, 129.7, 130.0, 131.2, 132.8, 148.4, 163.0, 163.8, 172.7; MS (ESI-) m/z : 363 (M – K) (100 %). HRMS (ESI-) m/z calculated for $\text{C}_{15}\text{H}_{11}\text{N}_2\text{O}_7\text{S}$ (M – K) 363.0292, found 363.0271.

4-Amino-3-sulfo-N-(2-aminoethyl)-1,8-naphthalimide, potassium salt (12)

Synthesised using the same general procedure as for **6**, commencing with 4-amino-3-sulfo-1,8-naphthalic anhydride (potassium salt) and ethylenediamine. To suppress formation of the di-imide, a 10-fold excess of ethylenediamine was used. A yellow solid was obtained.

Yield 0.176 g (79 %); MP > 250 °C; $^1\text{H-NMR}$ δ 2.74 (2H, t, $J = 6.9$ Hz, H_2), 4.02 (2H, t, $J = 6.9$ Hz, H_1), 7.67 (1H, dd, $J = 7.2, 8.4$ Hz, H_6), 7.80 (2H, br s, NH_2), 8.41 (1H, dd, $J = 0.6, 7.2$ Hz, H_7), 8.60 (1H, s, H_2), 8.68 (1H, dd, $J = 0.6, 8.4$ Hz, H_5); $^{13}\text{C-NMR}$ δ 40.2, 42.5, 106.9, 120.8, 122.2, 124.7, 125.2, 129.7, 129.8, 131.2, 132.8, 148.2, 163.3, 164.1 ppm; MS (ESI-) m/z : 334 (M – K) (100 %); Elem. Anal. ($\text{C}_{14}\text{H}_{12}\text{KN}_3\text{O}_5\text{S}$): Calc. C 45.03, H 3.24, N 11.25; Found C 44.94, H 3.27, N 11.58.

4-Amino-3-sulfo-N-(2-(dimethylamino)ethyl)-1,8-naphthalimide, potassium salt (13)

Synthesised using the same general procedure as for **9**, commencing with 4-amino-3-sulfo-1,8-naphthalic anhydride, potassium salt (**3**) and *N,N*-dimethylethylenediamine. A yellow-brown solid was obtained.

Yield 0.160 g (66 %); MP > 250 °C; $^1\text{H NMR}$ δ 2.87 (6H, s), 3.40 (2H, t, $J = 5.7$ Hz), 4.34 (2H, t, $J = 5.7$ Hz), 7.71 (1H, dd, $J = 7.2, 8.4$ Hz), 7.89 (2H, br s, NH_2), 8.44 (1H, d, $J = 7.2$ Hz), 8.64 (1H, s), 8.73 (1H, d, $J = 8.4$ Hz); $^{13}\text{C NMR}$ δ 35.1, 43.1, 55.5, 106.6, 120.8, 122.0, 124.8, 125.1, 129.9, 130.2, 131.4, 133.1, 148.6, 163.6, 164.5; MS (ESI-) m/z : 362 (M – K) (100 %). HRMS (ESI-) m/z calculated for $\text{C}_{16}\text{H}_{16}\text{N}_3\text{O}_5\text{S}$ (M – K) 362.0816, found 362.0782.

4-Amino-3-sulfo-N-(2-(piperazin-1-yl)ethyl)-1,8-naphthalimide, potassium salt (14)

Synthesised using the same general procedure as for **9**, commencing with 4-amino-3-sulfo-1,8-naphthalic anhydride (potassium salt) and 1-(2-aminoethyl)piperazine. A yellow solid was obtained.

Yield 0.272 g (82 %); MP > 250 °C; $^1\text{H-NMR}$ δ 2.62 (6H, m, $\text{H}_2, \text{H}_3, \text{H}_6$), 3.01 (4H, m, H_4, H_5), 4.14 (2H, t, $J = 6.6$ Hz, H_1), 7.68 (1H, dd, $J = 7.5, 8.1$ Hz, H_6), 7.83 (2H, br s, NH_2), 8.41 (1H, dd, $J = 0.6, 7.5$ Hz, H_7), 8.62 (1H, s, H_2), 8.69 (1H, dd, $J = 0.6, 8.1$ Hz, H_5); $^{13}\text{C-NMR}$ δ 36.6, 43.4 (2C), 49.7 (2C),

55.2, 106.6, 120.8, 121.9, 124.8, 125.1, 129.7, 130.0, 131.3, 132.9, 148.4, 163.2 (C_{10}), 164.0 (C_9) ppm; MS (ESI-) m/z : 403 (M – K) (100 %); Elem. Anal. ($\text{C}_{18}\text{H}_{19}\text{N}_4\text{O}_5\text{S}$): Calc. C 53.59, H 4.75, N 13.89; Found C 53.67, H 4.78, N 13.88.

4-Amino-3-sulfo-N-phenyl-1,8-naphthalimide, potassium salt (15)

To a stirred suspension of 4-amino-3-sulfo-1,8-naphthalic anhydride, potassium salt (**3**) (0.197 g, 0.59 mmol), in aqueous acetic acid (5 %, 5 mL), was added aniline (0.069 g, 0.74 mmol). The reaction mixture was stirred at 120 °C for 18 hours, then diluted to 15 mL with hot water. Addition of KCl (~0.5 g), followed by cooling to 4 °C, resulted in precipitation of the product. The resulting suspension was then stored at 4 °C for 24 hours. The solid product was collected by filtration, washed sequentially with water, ethanol and ether, and dried under vacuum to afford the desired product as a yellow solid.

Yield 0.146 g (60 %); MP > 250 °C; $^1\text{H NMR}$ δ 7.31 (2H, m), 7.45 (3H, m), 7.71 (1H, dd, $J = 7.5, 8.1$ Hz), 7.87 (2H, br s, NH_2), 8.42 (1H, d, $J = 7.5$ Hz), 8.61 (1H, s), 8.74 (1H, d, $J = 8.1$ Hz); $^{13}\text{C NMR}$ δ 107.1, 121.0, 122.5, 124.8, 125.2, 128.0, 128.9, 129.4, 130.1, 131.3, 132.8, 136.7, 148.4, 163.4, 164.2. MS (ESI-) m/z : 367 (M – K) (100 %).

4-Amino-3-sulfo-N-(3-hydroxyphenyl)-1,8-naphthalimide, potassium salt (16)

Synthesised using the same general procedure as for **15**, commencing with 4-amino-3-sulfo-1,8-naphthalic anhydride (potassium salt) and 3-aminophenol. A yellow-brown solid was obtained.

Yield 0.164 g (65 %); MP > 250 °C; $^1\text{H NMR}$ δ 6.67 (1H, m) 6.70 (1H, m), 6.81 (1H, m), 7.26 (1H, t, $J = 8.1$ Hz), 7.70 (1H, dd, $J = 7.2, 8.4$ Hz), 7.86 (2H, br s, NH_2), 8.41 (1H, dd, $J = 1.2, 7.2$ Hz), 8.59 (1H, s), 8.73 (1H, dd, $J = 1.2, 8.4$ Hz), 9.60 (1H, br s, OH); $^{13}\text{C NMR}$ (100 MHz) δ 107.1, 115.1, 116.5, 119.9, 120.9, 122.5, 124.7, 125.2, 129.5, 130.0, 130.1, 131.3, 132.8, 137.6, 148.4, 157.9, 163.2, 164.0; MS (ESI-) m/z : 383 (M – K) (100 %).

4-Amino-3-sulfo-N-(4-hydroxyphenyl)-1,8-naphthalimide, potassium salt (17)

Synthesised using the same general procedure as for **15**, commencing with 4-amino-3-sulfo-1,8-naphthalic anhydride, potassium salt (**3**) and 4-aminophenol. A brown solid was obtained.

Yield 0.179 g (70 %); MP > 250 °C; $^1\text{H NMR}$ ($\text{DMSO-}d_6$) δ 6.83 (2H, d, $J = 8.7$ Hz), 7.05 (2H, d, $J = 8.7$ Hz), 7.69 (1H, dd, $J = 7.2, 8.4$ Hz), 7.81 (2H, br s, NH_2), 8.41 (1H, dd, $J = 1.2, 7.2$ Hz), 8.61 (1H, s), 8.71 (1H, dd, $J = 1.2, 8.4$ Hz), 9.53 (1H, br s, OH); $^{13}\text{C NMR}$ ($\text{DMSO-}d_6$) δ 107.2, 115.5, 121.0, 122.6, 124.8, 125.1, 127.6, 130.0, 130.1, 130.2, 131.4, 132.8, 148.3, 157.1, 163.6, 164.4; MS (ESI-) m/z : 383 (M – K) (100 %).

4-Amino-3-sulfo-N-(4-methoxyphenyl)-1,8-naphthalimide, potassium salt (18)

Synthesised using the same general procedure as for **15**, commencing with 4-amino-3-sulfo-1,8-naphthalic anhydride,

potassium salt (**3**) and 4-methoxyaniline. A brown solid was obtained.

Yield 0.165 g (77 %); MP > 250 °C; ^1H NMR (DMSO- d_6) δ 3.82 (1H, s, 3H), 6.91 (2H, d, J = 8.5 Hz), 7.08 (2H, d, J = 8.5 Hz), 7.81 (1H, dd, J = 7.3, 8.2 Hz), 7.71 (2H, br s, NH₂), 8.23 (1H, dd, J = 1.2, 7.2 Hz), 8.58 (1H, s), 8.94 (1H, dd, J = 1.2, 8.4 Hz); ^{13}C NMR (DMSO- d_6) δ 54.8, 106.3, 117.5, 119.7, 121.6, 123.5, 126.3, 126.9, 130.2, 130.7, 131.2, 133.4, 134.2, 152.3, 161.1, 167.6, 168.4; MS (ESI-) m/z : 397 (M – K) (100 %). HRMS (ESI-) m/z calculated for C₁₉H₁₃N₂O₆S (M – K) 397.0500, found 397.0521.

4-Amino-3-sulfo-N-(3-hydroxypropyl)-1,8-naphthalimide, potassium salt (19)

Synthesised using the same general procedure as for **6**, commencing with 4-amino-3-sulfo-1,8-naphthalic anhydride, potassium salt (**3**) and 3-amino-1-propanol. A yellow solid was obtained.

Yield 0.197 g (83 %); MP > 250 °C. ^1H NMR δ 1.74 (2H, m), 3.46 (2H, m), 4.06 (2H, t, J = 7.2 Hz), 4.48 (1H, t, J = 5.4 Hz, OH), 7.68 (1H, dd, J = 7.2, 8.4 Hz), 7.80 (2H, br s, NH₂), 8.42 (1H, dd, J = 0.6, 7.2 Hz), 8.61 (1H, s), 8.68 (1H, dd, J = 0.6, 8.4 Hz); ^{13}C NMR δ 31.4, 37.4, 59.3, 106.9, 120.9, 122.1, 124.9, 125.0, 129.7, 130.0, 131.4, 132.9, 148.4, 163.3, 164.0; MS (ESI-) m/z : 349 (M – K) (100 %). HRMS (ESI-) m/z calculated for C₁₅H₁₃N₂O₆S (M – K) 349.0500, found 349.0492.

4-Amino-3-sulfo-N-(5-hydroxypentyl)-1,8-naphthalimide, potassium salt (20)

Synthesised using the same general procedure as for **6**, commencing with 4-amino-3-sulfo-1,8-naphthalic anhydride (potassium salt) and 5-amino-1-pentanol. A yellow solid was obtained.

Yield 0.270 g (84 %); MP > 250 °C; ^1H -NMR δ 1.33 (2H, m), 1.45 (2H, m), 1.59 (2H, m), 3.36 (2H, m), 3.99 (2H, t, J = 7.2 Hz), 4.34 (1H, t, J = 5.1 Hz, OH), 7.68 (1H, dd, J = 7.5, 8.1 Hz), 7.81 (2H, br s, NH₂), 8.42 (1H, d, J = 7.5 Hz), 8.60 (1H, s), 8.68 (1H, d, J = 8.1 Hz); ^{13}C -NMR δ 23.3, 27.8, 32.5, 39.5, 60.7, 106.8, 120.8, 122.0, 124.8, 125.1, 129.6, 129.9, 131.3, 132.8, 148.3, 163.1, 163.9; MS (ESI-) m/z : 377 (M – K) (100 %). HRMS (ESI-) m/z calculated for C₁₇H₁₇N₂O₆S (M – K) 377.0813, found 377.0839.

4-Amino-3-sulfo-N-(5-hydroxyhexyl)-1,8-naphthalimide, potassium salt (21)

Synthesised using the same general procedure as for **6**, commencing with 4-amino-3-sulfo-1,8-naphthalic anhydride (potassium salt) and 6-amino-1-hexanol. A brown solid was obtained.

Yield 0.165 g (74 %); MP > 250 °C; ^1H -NMR δ 1.29 (2H, m), 1.43 (2H, m), 1.67 (2H, m), 1.58 (2H, m), 3.14 (2H, m), 3.62 (2H, m), 4.70 (1H, bm), 5.32 (2H, bs, NH₂), 7.92 (1H, dd, J = 7.5, 8.0 Hz), 8.28 (1H, d, J = 7.5 Hz), 8.45 (1H, s), 8.57 (1H, d, J = 8.0 Hz); ^{13}C -NMR δ 24.2, 26.7, 30.2, 32.5, 40.4, 61.7, 108.8, 120.7, 127.3, 129.4, 130.1, 132.6, 132.9, 134.0, 137.5, 148.7, 164.7, 165.2; MS (ESI-) m/z : 391 (M – K) (100

%). HRMS (ESI-) m/z calculated for C₁₈H₁₉N₂O₆S (M – K) 391.0969, found 391.0955.

4-Amino-3-sulfo-N-(2-mercaptoethyl)-1,8-naphthalimide, potassium salt (22)

Synthesised using the same general procedure as for **9**, commencing with 4-amino-3-sulfo-1,8-naphthalic anhydride, potassium salt (**3**) and cysteamine. A yellow solid was obtained.

Yield 0.245 g (82 %); MP > 250 °C. ^1H NMR (DMSO- d_6) δ 2.96 (2H, m), 4.31 (2H, m), 7.69 (1H, dd, J = 7.2, 8.4 Hz), 7.84 (2H, br s, NH₂), 8.43 (1H, d, J = 7.2 Hz), 8.61 (1H, s), 8.70 (1H, d, J = 8.4 Hz); ^{13}C NMR (DMSO- d_6) δ 35.2, 38.2, 106.5, 120.8, 121.8, 124.8, 125.1, 129.7, 130.1, 131.4, 133.0, 148.5, 163.0, 163.9; MS (ESI-) m/z : 351 (M – K). HRMS (ESI-) m/z calculated for C₁₄H₁₁N₂O₅S₂ (M – K) 351.0115, found 351.0121.

4-Amino-3-sulfo-N-(carboxymethyl)-1,8-naphthalimide, potassium salt (23)

Glycine (0.089 g, 1.19 mmol) was added to a stirring suspension of 4-amino-3-sulfo-1,8-naphthalic anhydride, potassium salt (**3**) (0.202 g, 0.61 mmol) in 1M Li⁺/H⁺ acetate buffer (pH 5, 5mL). After stirring at 120 °C for 18 hours, the resulting solution was diluted with water, to a volume of 15 mL. The diluted reaction mixture was then acidified with concentrated HCl (pH 3), and the product salted out by addition of KCl (~0.5 g). The reaction mixture was allowed to stand at 4 °C for 24 hours to increase precipitation of the product. The product was collected by filtration, washed sequentially with cold water, ethanol and ether, and dried under vacuum. An orange-brown solid was obtained.

Yield 0.151 g (64 %); MP > 250 °C; ^1H NMR δ 4.68 (2H, s), 7.71 (1H, dd, J = 7.2, 8.4 Hz), 7.88 (2H, br s, NH₂), 8.44 (1H, d, J = 7.2 Hz), 8.61 (1H, s), 8.75 (1H, d, J = 8.4 Hz); ^{13}C NMR δ 41.1, 106.1, 120.9, 121.6, 124.8, 125.2, 129.8, 130.4, 131.6, 133.0, 148.8, 162.7, 163.7, 169.9; MS (ESI-) m/z : 349 (M – K) (100 %); Elem. Anal. (C₁₄H₁₁KN₂O₈S.H₂O): Calc. C 41.38, H 2.73, N 6.89; Found C 41.35, H 2.78, N 6.92.

4-Amino-3-sulfo-N-benzyl-1,8-naphthalimide, potassium salt (24)

Synthesised using the same general procedure as for **9**, commencing with 4-amino-3-sulfo-1,8-naphthalic anhydride, potassium salt (**3**) and benzylamine. A yellow solid was obtained.

Yield 0.148 g (60 %); MP > 250 °C; ^1H NMR δ 5.31 (2H, s), 7.24 (5H, m), 7.69 (1H, dd, J = 7.2, 8.4 Hz), 7.87 (2H, br s, NH₂), 8.43 (1H, d, J = 7.2 Hz), 8.63 (1H, s), 8.71 (1H, d, J = 8.4 Hz); ^{13}C NMR δ 42.7, 106.5, 120.8, 121.9, 124.8, 125.2, 127.0, 127.6, 128.5, 129.8, 130.2, 131.5, 133.1, 138.1, 148.6, 163.2, 163.9; MS (ESI-) m/z : 381 (M – K) (100 %).

4-Amino-3-sulfo-N-(2-aminobenzyl)-1,8-naphthalimide, potassium salt (25)

To a stirring suspension of 4-amino-3-sulfo-1,8-naphthalic anhydride, potassium salt (**3**) (0.200 g, 0.60 mmol) in ethanol (7 mL), was added TEA (3 drops) and 2-aminobenzylamine

(0.221 g, 1.81 mmol). A 3-fold excess of 2-aminobenzylamine was used to minimise formation of the di-imide. The resulting yellow-orange suspension was stirred at 100 °C for 18 hours, then cooled to room temperature with stirring. The yellow product was collected by filtration, washed sequentially with ethanol and ether, and dried under vacuum. A bright yellow solid was obtained.

Yield 0.262 g (100 %); MP > 250 °C; ¹H NMR (DMSO-*d*₆) δ 5.04 (2H, s), 5.20 (2H, br s, NH₂), 6.42 (1H, m), 6.63 (1H, m), 6.90 (1H, m), 6.91 (1H, m), 7.70 (1H, dd, *J* = 7.2, 8.4 Hz), 7.88 (1H, br s, NH₂), 8.45 (1H, dd, *J* = 0.9, 7.2 Hz), 8.65 (1H, s), 8.72 (1H, dd, *J* = 0.9, 8.4 Hz); ¹³C NMR (DMSO-*d*₆) δ 39.7, 106.4, 115.0, 116.1, 120.4, 120.8, 121.9, 124.8, 125.3, 127.7, 128.2, 129.7, 130.2, 131.6, 133.2, 146.4, 148.6, 163.5, 164.2 ppm; MS (ESI-) *m/z*: 396 (M – K) (100 %).

4-Amino-3-sulfo-N-(3-aminobenzyl)-1,8-naphthalimide, potassium salt (26)

Synthesised using the same general procedure as for **25**, commencing with 4-amino-3-sulfo-1,8-naphthalic anhydride (potassium salt) and 3-aminobenzylamine. A yellow solid was obtained.

Yield 0.209 g (79 %); MP > 250 °C; ¹H NMR (DMSO-*d*₆) δ 4.95 (2H, br s, NH₂), 5.08 (2H, s), 6.37 (1H, dd, *J* = 1.8, 7.8 Hz), 6.42 (1H, d, *J* = 1.8 Hz), 6.45 (1H, d, *J* = 7.8 Hz), 6.90 (1H, t, *J* = 7.8 Hz), 7.69 (1H, dd, *J* = 7.2, 8.4 Hz), 7.85 (2H, br s, NH₂), 8.43 (1H, dd, *J* = 0.9, 7.2 Hz), 8.64 (1H, s), 8.71 (1H, dd, *J* = 0.9, 8.4 Hz); ¹³C NMR δ 42.7, 106.6, 112.3, 112.5, 115.0, 120.8, 122.0, 124.8, 125.2, 128.9, 129.7, 130.1, 131.4, 133.1, 138.6, 148.5, 148.9, 163.1, 163.8 ppm; MS (ESI-) *m/z*: 396 (M – K) (100 %); Elem. Anal. (C₁₉H₁₄KN₃O₅S.2H₂O): Calc. C 48.40, H 3.85, N 8.91; Found C 48.37, H 3.78, N 8.92.

4-Amino-3-sulfo-N-(4-aminobenzyl)-1,8-naphthalimide, potassium salt (27)

Synthesised using the same general procedure as for **25**, commencing with 4-amino-3-sulfo-1,8-naphthalic anhydride, potassium salt (**3**) and 4-aminobenzylamine. A bright yellow solid was obtained.

Yield 0.245 g (94 %); MP > 250 °C;⁴⁷ ¹H NMR δ 4.92 (2H, br s, NH₂), 5.02 (2H, s), 6.45 (2H, d, *J* = 8.4 Hz), 7.04 (2H, d, *J* = 8.4 Hz), 7.68 (1H, dd, *J* = 7.2, 8.4 Hz), 7.82 (2H, br s, NH₂), 8.42 (1H, dd, *J* = 1.2, 7.2 Hz), 8.63 (1H, s), 8.68 (1H, dd, *J* = 1.2, 8.4 Hz); ¹³C NMR δ 42.3, 106.8, 113.8, 120.8, 122.1, 124.8, 125.1, 125.2, 129.2, 129.6, 130.0, 131.4, 133.0, 147.8, 148.4, 163.2, 163.9 ppm; MS (ESI-) *m/z*: 396 (M – K) (100 %).

4-Amino-3-sulfo-N-(4-hydroxybenzyl)-1,8-naphthalimide, potassium salt (28)

Synthesised using the same general procedure as for **9**, commencing with 4-amino-3-sulfo-1,8-naphthalic anhydride (potassium salt) and 4-hydroxybenzylamine. A yellow-brown solid was obtained.

Yield 0.081 g (31 %); MP 242-244 °C; ¹H NMR δ 5.09 (2H, s), 6.65 (2H, d, *J* = 8.4 Hz), 7.16 (2H, d, *J* = 8.4 Hz), 7.68 (1H, dd, *J* = 7.2, 8.4 Hz), 7.83 (2H, br s, NH₂), 8.42 (1H, dd, *J* = 1.2, 7.2 Hz), 8.63 (1H, s), 8.69 (1H, dd, *J* = 1.2, 8.4 Hz), 9.25

(1H, br s, OH); ¹³C NMR δ 42.1, 106.6, 115.2, 120.8, 122.0, 124.8, 125.2, 128.4, 129.4, 129.7, 130.0, 131.4, 133.0, 148.5, 156.5, 163.1, 163.9 ppm; MS (ESI-) *m/z*: 397 (M – K) (100 %).

4-Amino-3-sulfo-N-(4-carboxybenzyl)-1,8-naphthalimide, potassium salt (29)

Synthesised using the same general procedure as for **9**, commencing with 4-amino-3-sulfo-1,8-naphthalic anhydride, potassium salt (**3**) and 4-(aminomethyl)benzoic acid. Total reaction time was 72 hours. An orange-brown solid was obtained.

Yield 0.133 g (48 %); MP > 250 °C; ¹H-NMR (DMSO-*d*₆) δ 5.26 (2H, s), 7.35 (2H, d, *J* = 8.4 Hz), 7.69 (1H, dd, *J* = 7.2, 8.4 Hz), 7.83 (2H, d, *J* = 8.4 Hz), 7.88 (2H, br s, NH₂), 8.44 (1H, dd, *J* = 1.2, 7.2 Hz), 8.64 (1H, s), 8.72 (1H, dd, *J* = 1.2, 8.4 Hz). ¹³C-NMR (DMSO-*d*₆) δ 42.6, 106.5, 120.9, 121.8, 124.8, 125.2, 127.2, 129.5, 129.8, 130.2, 131.6, 131.8, 133.1, 142.1, 148.6, 163.1, 164.0, 167.8; MS (ESI-) *m/z*: 425 (M – K) (100 %). HRMS (ESI-) *m/z* calculated for C₂₀H₁₃N₂O₇S (M – K) 425.0449, found 425.0451.

4-Amino-3-sulfo-N-(phenethyl)-1,8-naphthalimide, potassium salt (30)

Synthesised using the same general procedure as for **9**, commencing with 4-amino-3-sulfo-1,8-naphthalic anhydride, potassium salt (**3**) and phenethylamine. A yellow-grey solid was obtained.

Yield 0.126 g (47 %); MP > 250 °C; ¹H NMR (DMSO-*d*₆) δ 2.90 (2H, m), 4.23 (2H, m), 7.22 (5H, m), 7.68 (1H, dd, *J* = 7.2, 8.4 Hz), 7.81 (2H, br s, NH₂), 8.42 (1H, dd, *J* = 1.2, 7.2 Hz), 8.62 (1H, s), 8.69 (1H, dd, *J* = 1.2, 8.4 Hz); ¹³C NMR (DMSO-*d*₆) δ 33.8, 40.8, 106.7, 120.8, 122.0, 124.7, 125.2, 126.4, 128.6, 128.8, 129.6, 129.9, 131.2, 132.8, 139.1, 148.4, 163.0, 163.8; MS (ESI-) *m/z*: 395 (M – K) (100 %).

Acknowledgements

The authors acknowledge the financial support of the Australian Research Council, the National Health and Medical Research Council (Australia), the Ramaciotti Foundation and the Australian Cancer Research Foundation.

Author Statement

The authors declare the following competing financial interest(s): We have entered into a commercial agreement with Abcam (Cambridge, UK) for the supply of some of our lead dynamin and clathrin inhibitors. This includes some of the compounds listed in this paper.

Notes and references

^a Centre for Chemical Biology, Chemistry, School of Environmental and Life Sciences, The University of Newcastle, Callaghan, NSW 2308, Australia. Phone: +61 29 216486; Fax: +61 29 215472; E-mail: Adam.McCluskey@newcastle.edu.au

^b Children's Medical Research Institute, 214 Hawkesbury Road, Westmead NSW 2145, Australia.

[†] Present Address: Organic Pharmaceutical Chemistry, Department of Medicinal Chemistry, Uppsala Biomedical Centre, Uppsala University,

Box 574, SE-751 23 Uppsala, Sweden. Fax: +46 18 4714474; Tel: +46 18 4714667

Electronic Supplementary Information (ESI) available: [details of any supplementary information available should be included here]. See DOI: 10.1039/b000000x/

1. S. M. Ferguson and P. De Camilli, *Nat. Rev. Mol. Cell Biol.*, 2012, **13**, 75-88.
2. R. M. Boumil, V. A. Letts, M. C. Roberts, C. Lenz, C. L. Mahaffey, Z.-w. Zhang, T. Moser and W. N. Frankel, *PLoS Genet.*, 2010, **6**, e1001046.
3. S. A. Pathan, G. K. Jain, S. Akhter, D. Vohora, F. J. Ahmad and R. K. Khar, *Drug Discov. Today*, 2010, **15**, 717-732.
4. S. Chaumont, C. André, D. Perrais, E. Boué-Grabot, A. Taly and M. Garret, *J. Biol. Chem.*, 2013, **288**, 28254-28265.
5. P. P. Eleniste, S. Huang, K. Wayakanon, H. W. Largura and A. Bruzzaniti, *Int. J. Biochem. Cell Biol.*, 2014, **46**, 9-18.
6. A. Bruzzaniti, L. Neff, A. Sanjay, W. C. Horne, P. De Camilli and R. Baron, *Mol. Biol. Cell*, 2005, **16**, 3301-3313.
7. M. T. F. Wolf, X.-R. Wu and C.-L. Huang, *Kidney Int.*, 2013, **84**, 130-137.
8. K. Soda, D. M. Balkin, S. M. Ferguson, S. Paradise, I. Milosevic, S. Giovedi, L. Volpicelli-Daley, X. Tian, Y. Wu, H. Ma, S. H. Son, R. Zheng, G. Moeckel, O. Cremona, L. B. Holzman, P. De Camilli and S. Ishibe, *J. Clin. Invest.*, 2012, **122**, 4401-4411.
9. C. B. Harper, M. R. Popoff, A. McCluskey, P. J. Robinson and F. A. Meunier, *Trends Cell Biol.*, 2013, **23**, 90-101.
10. Y. Sun and P. Tien, *Crit. Rev. Microbiol.*, 2013, **39**, 166-179.
11. J. S. Chappie, J. A. Mears, S. Fang, M. Leonard, S. L. Schmid, R. A. Milligan, J. E. Hinshaw and F. Dyda, *Cell*, 2011, **147**, 209-222.
12. B. Marks, M. H. B. Stowell, Y. Vallis, I. G. Mills, A. Gibson, C. R. Hopkins and H. T. McMahon, *Nature*, 2001, **410**, 231-235.
13. G. J. K. Praefcke and H. T. McMahon, *Nat. Rev. Mol. Cell Biol.*, 2004, **5**, 133-147.
14. S. Sever, A. B. Muhlberg and S. L. Schmid, *Nature*, 1999, **398**, 481-486.
15. S. L. Schmid and V. A. Frolov, *Annu. Rev. Cell. Dev. Biol.*, 2011, **27**, 79-105.
16. K. Faelber, M. Held, S. Gao, Y. Posor, V. Haucke, F. Noé and O. Daumke, *Structure*, 2012, **20**, 1621-1628.
17. S. M. Ferguson, G. Brasnjo, M. Hayashi, M. Wölfel, C. Collesi, S. Giovedi, A. Raimondi, L.-W. Gong, P. Ariel, S. Paradise, E. O'Toole, R. Flavell, O. Cremona, G. Miesenböck, T. A. Ryan and P. De Camilli, *Science*, 2007, **316**, 570-574.
18. Y.-W. Liu, M. C. Surka, T. Schroeter, V. Lukiyanchuk and S. L. Schmid, *Mol. Biol. Cell*, 2008, **19**, 5347-5359.
19. A. Raimondi, Shawn M. Ferguson, X. Lou, M. Armbruster, S. Paradise, S. Giovedi, M. Messa, N. Kono, J. Takasaki, V. Cappello, E. O'Toole, Timothy A. Ryan and P. De Camilli, *Neuron*, 2011, **70**, 1100-1114.
20. A. Quan, A. B. McGeachie, D. J. Keating, E. M. van Dam, J. Rusak, N. Chau, C. S. Malladi, C. Chen, A. McCluskey, M. A. Cousin and P. J. Robinson, *Mol. Pharmacol.*, 2007, **72**, 1425-1439.
21. T. Hill, L. R. Odell, J. K. Edwards, M. E. Graham, A. B. McGeachie, J. Rusak, A. Quan, R. Abagyan, J. L. Scott, P. J. Robinson and A. McCluskey, *J. Med. Chem.*, 2005, **48**, 7781-7788.
22. L. R. Odell, N. Chau, A. Mariana, M. E. Graham, P. J. Robinson and A. McCluskey, *ChemMedChem*, 2009, **4**, 1182-1188.
23. J. Zhang, G. A. Lawrance, N. Chau, P. J. Robinson and A. McCluskey, *New J. Chem.*, 2008, **32**, 28-36.
24. T. A. Hill, A. Mariana, C. P. Gordon, L. R. Odell, M. J. Robertson, A. B. McGeachie, N. Chau, J. A. Daniel, N. N. Gorgani, P. J. Robinson and A. McCluskey, *J. Med. Chem.*, 2010, **53**, 4094-4102.
25. L. R. Odell, D. Howan, C. P. Gordon, M. J. Robertson, N. Chau, A. Mariana, A. E. Whiting, R. Abagyan, J. A. Daniel, N. N. Gorgani, P. J. Robinson and A. McCluskey, *J. Med. Chem.*, 2010, **53**, 5267-5280.
26. C. B. Harper, S. Martin, T. H. Nguyen, S. J. Daniels, N. A. Lavidis, M. R. Popoff, G. Hadzic, A. Mariana, N. Chau, A. McCluskey, P. J. Robinson and F. A. Meunier, *J. Biol. Chem.*, 2011, **286**, 35966-35976.
27. A. McCluskey, J. A. Daniel, G. Hadzic, N. Chau, E. L. Clayton, A. Mariana, A. Whiting, N. N. Gorgani, J. Lloyd, A. Quan, L. Moshkanbaryans, S. Krishnan, S. Perera, M. Chircop, L. von Kleist, A. B. McGeachie, M. T. Howes, R. G. Parton, M. Campbell, J. A. Sakoff, X. Wang, J.-Y. Sun, M. J. Robertson, F. M. Deane, T. H. Nguyen, F. A. Meunier, M. A. Cousin and P. J. Robinson, *Traffic*, 2013, **14**, 1272-1289.
28. M. J. Robertson, G. Hadzic, J. Ambrus, D. Y. Pomè, E. Hyde, A. Whiting, A. Mariana, L. von Kleist, N. Chau, V. Haucke, P. J. Robinson and A. McCluskey, *ACS Med. Chem. Lett.*, 2012, **3**, 352-356.
29. K. A. MacGregor, M. K. Abdel-Hamid, L. R. Odell, N. Chau, A. Whiting, P. J. Robinson and A. McCluskey, *Eur. J. Med. Chem.*, 2014, **85**, 191-206.
30. T. A. Hill, C. P. Gordon, A. B. McGeachie, B. Venn-Brown, L. R. Odell, N. Chau, A. Quan, A. Mariana, J. A. Sakoff, M. Chircop, P. J. Robinson and A. McCluskey, *J. Med. Chem.*, 2009, **52**, 3762-3773.
31. C. P. Gordon, B. Venn-Brown, M. J. Robertson, K. A. Young, N. Chau, A. Mariana, A. Whiting, M. Chircop, P. J. Robinson and A. McCluskey, *J. Med. Chem.*, 2012, **56**, 46-59.
32. J. A. Daniel, N. Chau, M. K. Abdel-Hamid, L. Hu, L. von Kleist, A. Whiting, S. Krishnan, P. Maamary, S. R. Joseph, F. Simpson, V. Haucke, A. McCluskey, and P. J. Robinson, *Traffic*, 2015, doi: 10.1111/tra.12272
33. M. J. Robertson, F. M. Deane, P. J. Robinson and A. McCluskey, *Nat. Protocols*, 2014, **9**, 851-870.
34. M. K. Haider, H.-O. Bertrand and R. E. Hubbard, *J. Chem. Infor. Mod.*, 2011, **51**, 1092-1105.
35. S. D. Larsen, T. Barf, C. Liljebriis, P. D. May, D. Ogg, T. J. O'Sullivan, B. J. Palazuk, H. J. Schostarez, F. C. Stevens and J. E. Bleasdale, *J. Med. Chem.*, 2001, **45**, 598-622.
36. M. Hussain, V. Ahmed, B. Hill, Z. Ahmed and S. D. Taylor, *Bioorganic & Medicinal Chemistry*, 2008, **16**, 6764-6777.
37. T. S. Elliott, A. Slowey, Y. Ye and S. J. Conway, *MedChemComm*, 2012, **3**, 735-751.
38. X. Huang, S. Huang, B. Zhai, Y. Zhang, Y. Xu and Q. Wang, *Tetrahedron Lett.*, 2012, **53**, 6414-6417.
39. E. A. Nothnagel, *Biochim. Biophys. Acta*, 1989, **980**, 209-219.
40. Chemical Computing Group Inc., 1010 Sherbooke St. West, Suite 910, Montreal, QC, Canada, 2012, vol. 2012.10.
41. J. S. Chappie, S. Acharya, M. Leonard, S. L. Schmid and F. Dyda, *Nature*, 2010, **465**, 435-440.

42. A. Levitzki, *Annu. Rev. Pharmacol. Toxicol.*, 2013, **53**, 161-185.
43. A. Quan and P. J. Robinson, in *Methods Enzymol.*, eds. C. J. D. William E. Balch and H. Alan, Academic Press, 2005, vol. **404**, pp. 556-569.
44. S. K. Ghosh, S. U. Hossain, S. Bhattacharya and S. C. Bhattacharya, *J. Photochem. Photobiol. B: Biol.*, 2005, **81**, 121-128.
45. H.-Q. Li, Z.-Q. Jiang, X. Wang, Y. Pan, F. Wang and S.-Q. Yu, *Res. Chem. Intermed.*, 2004, **30**, 369-381.
46. L. D. Van Vliet, T. Ellis, P. J. Foley, L. Liu, F. M. Pfeffer, R. A. Russell, R. N. Warren, F. Hollfelder and M. J. Waring, *J. Med. Chem.*, 2007, **50**, 2326-2340.
47. K. A. MacGregor, M. J. Robertson, K. A. Young, L. von Kleist, W. Stahlschmidt, A. Whiting, N. Chau, P. J. Robinson, V. Haucke and A. McCluskey, *J. Med. Chem.*, 2013, **57**, 131-143.

1.